25th ABCM International Congress of Mechanical Engineering
October20-25, 2019, Uberlândia, MG, Brazil

MICROSTRUCTURAL AND MECHANICAL CHARACTERIZATION OF WE43 MAGNESIUM ALLOY

Gualter Silva Pereira
Gustavo Buldrini Teixeira
Waldek Wladimir Bose Filho
Department of Materials Engineering, São Carlos School of Engineering, University of SãoPaulo, 13566-590-São Carlos-SP, Brazil.
gualter@usp.br
gbuldrini@usp.br
waldek@sc.usp.br

Marcos Hideki Miyazaki
Fernando Fernandez
Brazilianaerospaceconglomerate, 12227-901 - São José dos Campos, SP - Brazil
marcos.miyazaki@embraer.com.br
fernando.fernandez@embraer.com.br

Julian A. Avila
UNESP – São Paulo State University, Campus of São João da Boa Vista, Av. Profª Isette Corrêa Fontão, 505, Jardim das Flores, 13876-750 - São João da Boa Vista, SP, Brazil.
julian.avila@unesp.br

The competition between thetransportation industries, such as astronautics, automotive, marine, and rail, drive toan incessant new designingof structures and parts. Also, the development and application of improved structural materials and processing with a wide spectrum of attractivemechanical characteristics have been implanted in modern products. New ultralight metallic alloys have been developed to replace the traditional ones, aimingweight reduction without significant compromising of the resistance. In this context, this work aimed to study the fatigue strength of the non-flammableWE43 magnesium alloy (Mg-Y-Nd-Zr). The microstructural evaluation by optical and scanning electron microscopies and fatigue tests for initiation and propagation lives were carried out. The microstructure results showedthe formation of α-Mg, $Mg_{41}Nd_5$and $Mg_{24}Y_5$ phases dispersed within and at boundaries of grains. The tensile and fatigue results showed similar behavior in both directions studied here (TL and LT), because of anisotropic microstructure.

Keywords: *Structural materials, Rare earth, Magnesium alloy WE43, Mechanical, Microstructure.*

1. INTRODUCTION

Magnesium (Mg) is an element with severaladvantages when compared to other light alloys, among them, Mg is one of the most abundant materials on earth and at sea; being 100% recyclable and having a low density of approximately 1.80g/cm3. Its alloys enable the production of parts with a weight reduction of up to 1/3 concerning similar aluminum alloys products, commonly used in the aeronautical industry. Mg alloys can be considered an innovative technology if applied for structural weight reduction, triggering sustainability in its various biases, such as economic, environmental, ecological and social (WENDT et al., 2014; KAINER, K. U. et al., 201; ESMAILY et al., 2017).

The high specific mechanical strength of Mg alloys makes them strong candidates to be chosen for light structural projects. However, due to its extraction and the little application in industry, the components produced from Mg alloys are more expensive than those produced from Al alloys. This lack of application is linked directly tothe absence of studies characterizing their microstructural and mechanical properties, causing the project engineers to choose more conventional materials. Therefore, detailed studies, correlating their microstructural features and mechanical properties, such as fracture toughness, fatigue, and corrosion resistance can expand the application possibilities, increasing the use and minimizing the cost of production (COY et al., 2010).

The most common Mg commercial alloys are AZ (Mg-Al-Zn) and AM (Mg-Al-Mn), they have unsatisfactory creep resistance at temperatures above 125 °C, flammability obstacles, lower mechanical and corrosion properties than Al alloys, restricting their applications in a larger scale in the fabrication of structural components. Recent studies have shown the effectiveness of adding rare earth elements and alkali metals in improving the creep, mechanical and corrosion resistance of Mg alloys. Among these mixed metals, we can highlight the non-flammable WE43 (Mg-Y-Nd-Zr) which the mechanical properties and corrosion resistance has been claimed to be superior to the AZ and AM alloys and can be

compared with some Al alloys used in the aeronautical industry (BLAWERT, 2004; CZERWINSKI, 2014; JIANG, H. S. et al, 2017; LIU, M. et al, 2012; MORDIKE, 2002; WANG et al., 2013; WENDT et al., 2005; ZUCCHI et al., 2007).

Rare earth elements (Yttrium and Neodymium) present in the WE43 alloy when subjected to temperatures above 25°C oxidize and form oxide layers (Nd_2O_3 and Y_2O_3) providing protection against flame initiation and propagation. Those rare earth elements exhibit good solubility in magnesium athigh temperatures, which declineif the temperature decreases, so that precipitation and aging hardening is made possible by supersaturated solution precipitation, thus forming thequais phases. These metastatic phases grow along the grain boundaries, improving theirmechanical properties (ZUCCHI et al., 2007; WANG et al., 2013). The addition of zirconium contributes to the grain refinement, due to the Zr network proximity parameter with Mg. If there is a good amount of zirconium alloys making it precipitates in the alloy, during its solidification, it forms points of heterogeneous nucleation (RZYCHOŃ et al., 2007; al., 2013).

The results presented here is part of a research project that aim to associate the effect of intrinsic (grain boundary orientation, crystallographic characteristics, precipitates, etc..) and extrinsic parameters (environment, galvanic contact, coatings) on the mechanical properties. The results presented here are related to some basic microstructure evaluation and fatigue results obtained in air environment of the WE43 Mg alloy.

2. EXPERIMENTAL

2.1 Material

The material used in this study was the magnesium alloy WE43C-T5 (Mg-Y-Nd-Zr), with aerospace specification AMS 4371, whose nominal composition is listed in the Table 1 below.

At the manufacturing process, this magnesium alloy plate was laminated and thermally treated (precipitation hardening) to the T5 condition, cooled and artificially aged. Test specimens were machined from Mg WE43C-T5 alloy in the directions TL, LT (L = main direction of deformation, T = less deformation direction) according to ASTM E399-12.

Table 1: Chemical composition of magnesium alloy WE43C-T5 (% Weight).

Elements	Minimum	Maximum
Mg	Bal.	
Y	3,7	4,3
Nd	2,0	2,5
Zr	0,2	1,0
Others	---	1,0

Source: EMBRAER - Brazilian Aerospace Conglomerate.

2.2 Optical microscopy and scanning electron microscopy (SEM)

Metallographic samples were prepared using nital 2% as etchant and examined in a Carl Zeiss ™ model AxioLab A1 optical microscope and a FEI® model FE-50 scanning electronic microscope (SEM). The preparation of the samples followed a strict protocol since they must be free of deformation and fine superficial layers of oxides, common in Mg alloys. Samples were ground using sandpaper till # 4000 and using alcohol as lubricant, followed by automated polishing with 10 N load and rotation of 160 RPM with diamond paste of 1 and 0.25 μm and finally, manual polishing with no load with OPS (colloidal silica).

2.3 X-ray diffraction (XRD)

X-ray diffraction (XRD) analysis were made in a Siemens D5005 system and the resultant diffractograms were evaluated through Oxford's Crystallographic Search-Match software.

2.4 Tensile Test

The tensile tests were performed following the ASTM E8M standard on round test specimens with 6 mm diameter and 38 mm gauge length, at room temperature (20˚C).

2.5 Fatigue resistance

Nucleation life, S-N curves

The S-N curves were obtained from round specimens, with tangentially blending fillets between the test section and the ends, with 7.5 mm in diameter and 25 mm gauge length, were removed transversally and longitudinally to the rolling direction. Fatigue test in load control was carried out following the ASTM E466, using a sinusoidal waveform, 15 Hz frequency and load ratios R= -1 and 0.1.

Propagation life, da/dN curves

Fatigue crack growth tests (FCG) followed the ASTM E647-13 standard and were performed in laboratory air conditions, at RT, constant amplitude load, sinusoidal waveform, frequency of 10 Hz and load ratio of 0.1 according to. For the FCG tests, CT-type specimens were extracted in the L-T and T-L directions. The FCG rates were obtained as a function of the variation of the stress intensity factor (ΔK) in the threshold and constant propagation regions (Paris). Size and geometry of the test specimens used in fatigue and FCG tests can be seen in Figure 1.

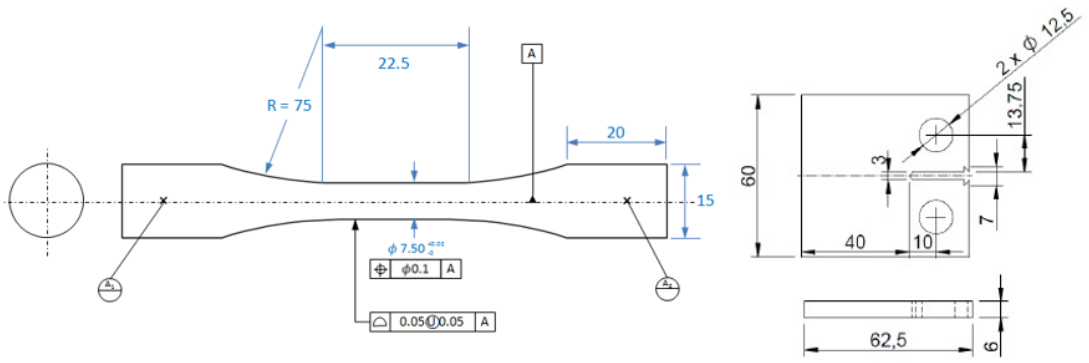

Figure 1: Size and geometry of the fatigue and FCG specimens.

3. RESULTS

3.1 Microstructural analysis

Figure 2 shows the microstructure of the WE43C-T5 alloy obtained by OM and SEM analysis, L-T plane (Fig. 2 a) MO and b) SEM) and S-L plane (Fig. 2 c) MO and d) SEM). It can be noticed a homogeneous microstructure with grain size of approximately 20 µm.

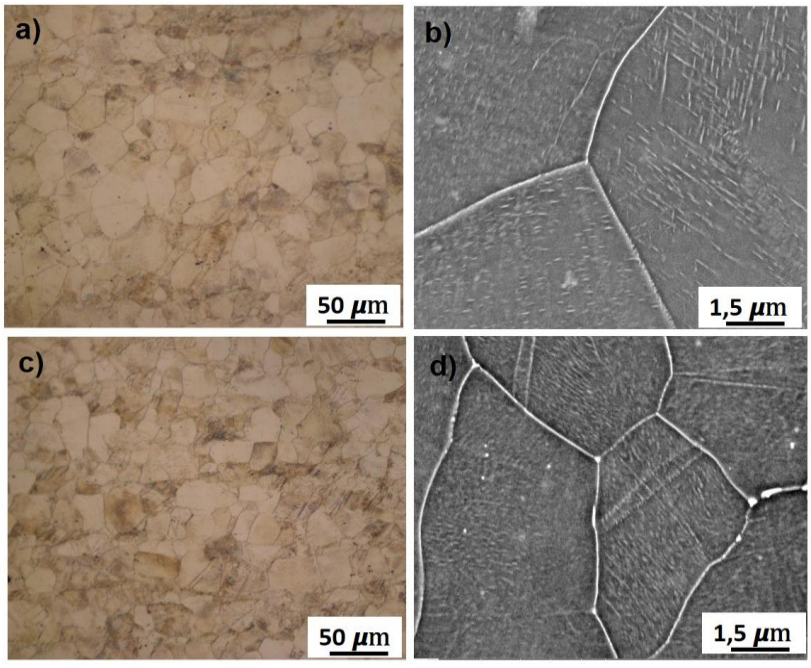

Figure 2: Microstructure of MgWE43C-T5 alloy obtained by OM and SEM analysis, a) and c) MO image in L-T and S-L planes respectively, b) and (d) SEM image, L-T and S-L planes respectively. Source: Elaborated by the author.

The SEM images show the dispersed precipitates inside the grains and at the grain boundaries. According to CHU (2015) and RIONTINO, (2006), these precipitates are probably intermetallic phases rich in Y and Nd. The resulting microstructure is due to the manufacturing process, and precipitation hardening occurred during the heat treatment involving three steps. First, the solubilization heat treatment, the alloy is submitted to an isothermal temperature of until its complete homogenization. During this stage, precipitates dissolve, and rare earth elements are positioned in a solid substitutional solution in the Mg crystal lattice. Second, quenching, rare earth elements keep their substitutional positions. Finally, during the artificial aging, a dispersion of the rare earth precipitates in the Mg matrixarise (ANTION et al., 2003; LI et al., 2016).

3.2 X-ray powder diffraction (XRD)

The diffractogram obtained using XRD of the WE43C-T5 alloy is shown in Fig. 3. After analysis, the specimen is composed of α-Mg, Mg41Nd5 e Mg24Y5.

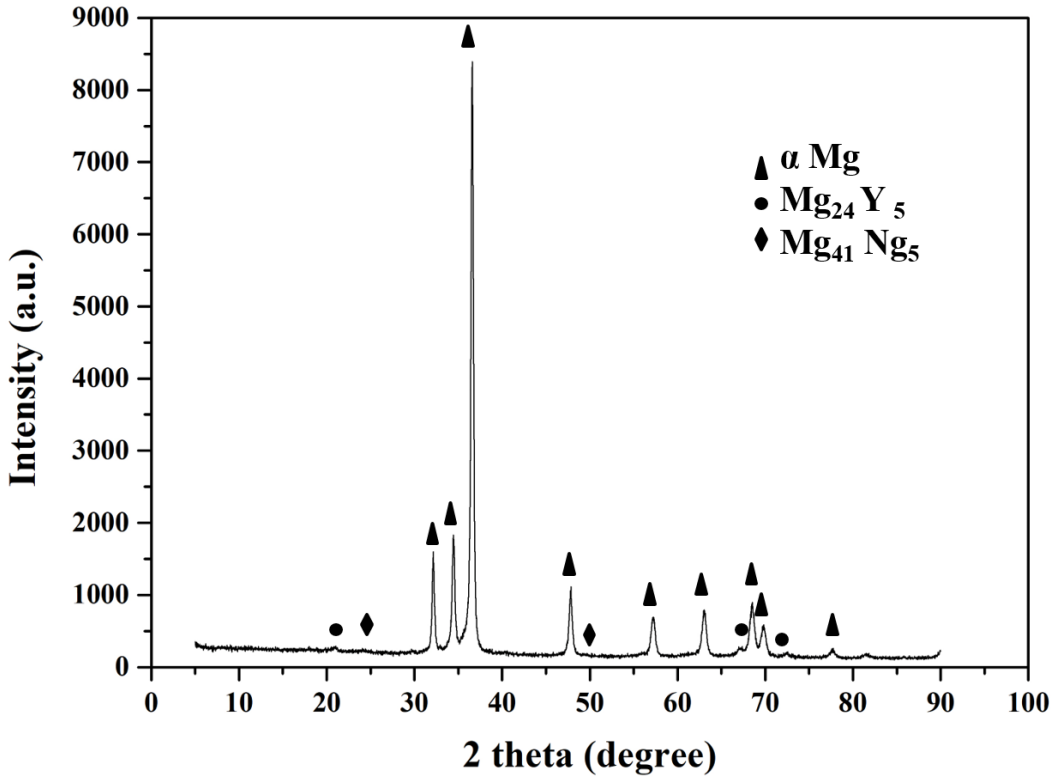

Figure 3: XRD diffractogram of WE43C-T5 alloy. Source: Elaborated by the author.

Some authors (MORDIKE, 2002; RZYCHOŃ; KIEŁBUS, 2007; SONG, 2005) attributed the excellent performance, stability of mechanical resistance up to 300 ° C, and corrosion resistance of the WE43 alloy in comparison to the other Mg alloys due to the formation of the phases shown above.

3.3 Tensile Testing

The Stress-Strain Test were made using 9 test specimens for each lamination plane, and the results are shown below in Figure 4 and Table 2.

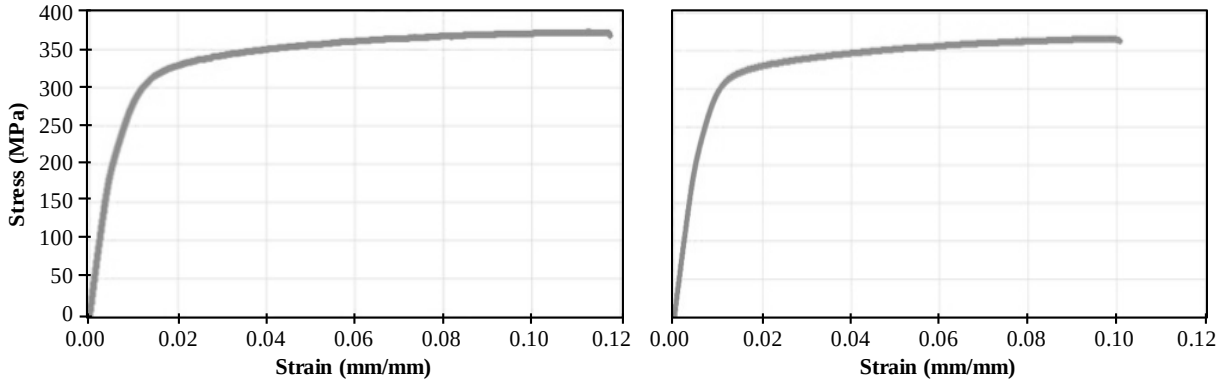

Figure 4: : Left: Tensile Test L-T. Right: Tensile Test T-L. Source: Elaborated by the author.

Table 2: Stress-Strain Test Results, Left L-T, and Right T-L.

Property	Specimen L	Specimen T
σ_y, MPa	268	246
σ_{UTS}, MPa	366	373
E, GPa	34,2	33,7

Source: Elaborated by the author.

Even though the microstructural analysis did not present a clear anisotropy, the tensile tests showed that the materials exhibit a certain amount of it, with the specimens removed with the centerline parallel to the rolling direction (specimen L) with higher values of tensile strength.

3.4 Fatigue

3.4.1 S-N Curves

Figure 5unveil the S-N results, and Table 3 presents the parameters of the S-N curves, $S_{max} = A.(N_f)^B$.

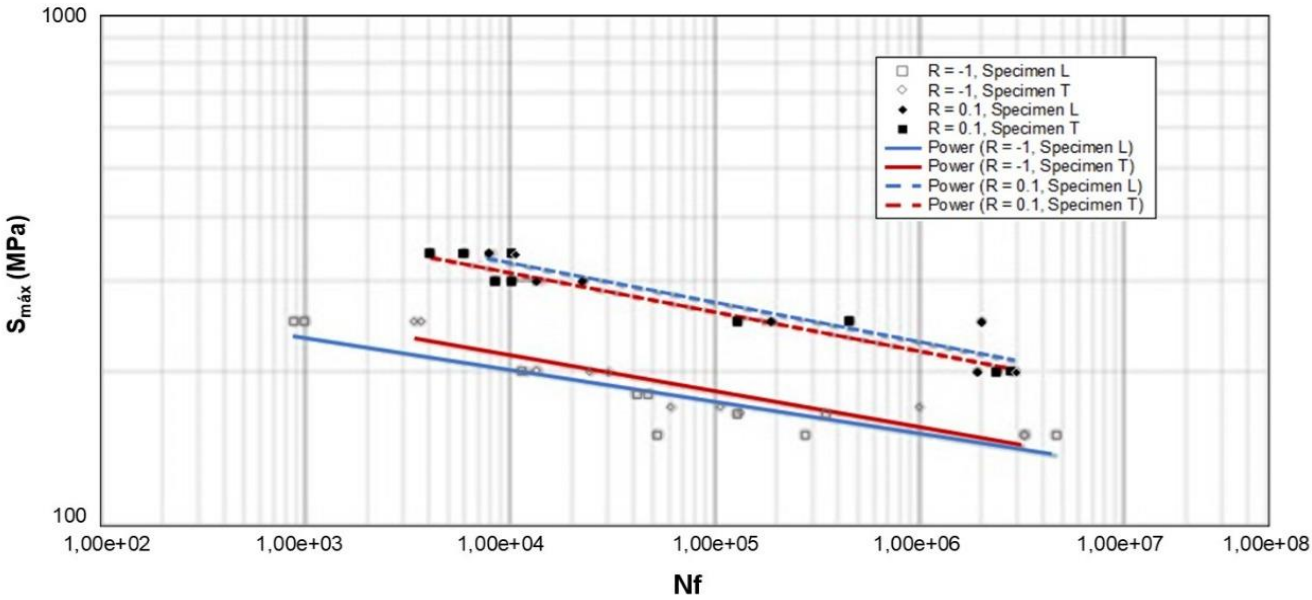

Figure 5: S-N curves, Smax = A.(Nf)B. Source: Elaborated by the author.

Table 2: Table 3: S-N curves parameters, Smax = A.(Nf)B.

R	Parameter	Specimen L	Specimen T
-1	A, MPa	411.1	358.1
	B	-0.071	-0.063
0.1	A, MPa	662.1	629.9
	B	-0.077	-0.077

Source: Elaborated by the author.

For the same applied R, it may be concluded that independent of the specimen direction the fatigue strength is quite similar; the materials did not exhibit a noticeable fatigue anisotropy. As expected, R= -1 has caused lower fatigue strength.

3.4.2 Fatigue crack propagation

Figure 6 shows the fatigue crack growth curves (da/dN) as a function of variation of the stress intensity factor applied ΔK, for the same test conditions, same load ratio (R = 0.1) in the L-T (red curve) and T-L (black curve) directions for the same test conditions. It was observed a similar fatigue resistance independently of the specimen direction.

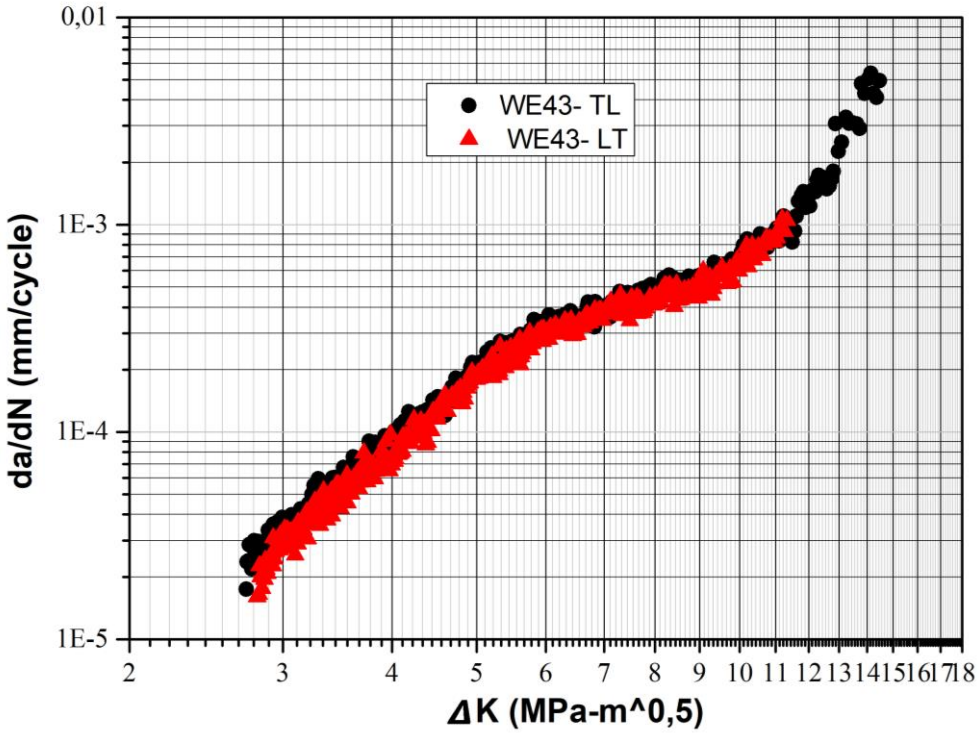

Figure 6: da/dNcurves (R = 0.1) in the L-T (red curve) and T-L (black curve). Source: Elaborated by the author.

As shown in Figure 2 a) and 2 c), WE43CMg-T5 alloy microstructures exhibit heterogeneous and equiaxed grains in both directions. The equiaxial structure is characterized by grain growth in different crystallographic directions, with no preference orientations, i.e.,the neighboring grains are not necessarily parallel to each other.

The crack propagation rate is strongly influenced by the microstructural arrangement of the metallic matrix, that is grain morphology and size, shape, and scattering of precipitates in the matrixVASUDEVAN et al. (1998).

The fatigue crack growth curves are quite similar. Table 4 shows the parameters of the Paris and Erdogan curve, and they are quite similar for both directions considered.

Table 4: Parameters m and C (are empirical constants of the material) and the equation of Paris.

Material	M	$\frac{C}{\frac{mm/ciclo}{(MPa\sqrt{m})^m}}$	Paris
WE 43- TL	1,40	2,62E-05	da/dN = 2,62E-05$(\Delta K)^{1,50}$
WE 43- LT	1,20	2,54E-05	da/dN =2,54E-05 $(\Delta K)^{120}$

Source: Elaborated by the author.

From each curve, the coefficient (m) and the linear coefficient (C) of the linear regression line of the Paris equation were determined. This model describes the fatigue behavior of the material only in region II and does not take into account the loading ratio R. This region is characterized by stable crack propagation where the log ratio of/dN versus log ΔK becomes linear. There was no significant difference in the values of the constant m, indicating that the crack propagation resistance is similar in both directions, but with the L-T direction being slightly more resistant to crack propagation than in the TL direction, as already observed in the Figure 3, which is due to factors directly related to the microstructure.

4. CONCLUSIONS

The formation of the α-Mg, $Mg_{41}Nd_5$, and $Mg_{24}Y_5$ phases present in the WE43C-T5 alloy were observed trough DRX analysis. The morphology of the equiaxed grains in the T-L and L-T planes are similar, and the precipitates are located dispersed in the contours and dispersed within the grains.

A slight anisotropy influence was observed in the tensile tests, which was not enough to cause any significant differences in the fatigue tests, with quite similar S-N fatigue results and crack propagation rate.

5. ACKNOWLEDGEMENTS

This study was financed in part by the Coordenação de Aperfeiçoamento de Pessoal de Nível Superior - Brasil (CAPES) - Finance Code 001 and EMBRAER which donated all the materials.

6. REFERENCES

Antion, C., et al., 2003. "Hardening precipitation in a Mg–4Y–3RE alloy." *Acta Materialia*, Vol. 51, pp. 5335–5348.

Blawert, C., Hort, N. and Kainer, K. U., 2004). "Automotive applications of magnesium and its alloys." *Trans. Indian Inst. Met*, Vol. 57, No. 4, pp 397-408.

Coy, A. E. et al., 2010. "Susceptibility of rare-earth-magnesium alloys to micro-galvanic corrosion". *Corrosion Science*, Vol. 52, No. 12, pp. 3896–3906.

Cui, Y. et al.,2015. "Enhanced damping capacity of magnesium alloys by tensile twin boundaries". *ScriptaMaterialia*, Vol. 101, pp. 8-11.

Czerwinski, F., 2014. "Controlling the ignition and flammability of magnesium for aerospace applications". *Corrosion Science*, Vol. 86, pp. 1–16.

Esmaily, M. et al., 2017. "Fundamentals and advances in magnesium alloy corrosion". *Progress in Materials Science*, Vol. 89, pp. 92–193.

Jiang, H. S. et al., 2017. "Microstructure and mechanical properties of WE43 magnesium alloy fabricated by direct-chill casting". *Materials Science and Engineering: A*, Vol. 684, pp. 158-164.

Li, H. et al., 2016. "Effect of heat treatment on microstructures and mechanical properties of a cast Mg-Y-Nd-Zr alloy". *Materials Science & Engineering A*, Vol. 667, pp. 409–416.

Liu, M. et al., 2012."The ignition temperature of Mg alloys WE43, AZ31 and AZ91". *Corrosion Science*, Vol. 54, No. 1, pp. 139–142.

Mordike, B. L., 2002. "Creep-resistant magnesium alloys". *Materials Science and Engineering A*, Vol. 324, No. 1–2, pp. 103–112.

Riontino, G.; Lussana, D.; Massazza, M. A., 2006. "A calorimetric study of phase evolution in a WE43 Mg alloy". *Journal of thermal analysis and calorimetry*, Vol. 83, No. 3, pp. 643-647.

Rzychoń, T.; Kiełbus, A., 2007. "Microstructure of WE43 casting magnesium alloy". *Journal of Achievements in Materials and Manufacturing Engineering*, Vol. 21, No. 1, pp. 31–34.

Song, G., 2005. "Recent progress in corrosion and protection of magnesium alloys". *Advanced Engineering Materials*, Vol. 7, No. 7, pp. 563–586.

Vasudevan, A. K.; Sadananda, K.; Rajan, K., 1998. "Role of microstructures on the growth of long fatigue cracks". *International journal of fatigue*. Vol. 19, No. 1, pp. 151–159.

Wang, X. et al., 2013. “Microstructure and mechanical properties of the hot-rolled Mg–Y–Nd–Zr alloy”. *Journal of Materials Research*, Vol. 28, No. 10, pp. 1386-1393.

Wendt, A. et al., 2005. “Magnesium Castings in Aeronautics Applications - Special Requirements”. *Essential Readings in Magnesium Technology*, pp. 65–69.

Zucchi, F. et al., 2006. “Electrochemical behaviour of a magnesium alloy containing rare earth elements”. *Journal of Applied Electrochemistry*, Vol. 36, No. 2, pp. 195-204.

7. RESPONSIBILITY NOTICE

The authorsare the only that responsible for the printed material included in this paper.